

Supplementary Information

Promoting CO₂ hydrogenation to light olefins over high-entropy oxide-supported Fe-based catalysts by turning the strong metal-support interaction

Zhijiang Ni^{a*}, Hanyu Shen^a, Lin Su^a, Xiaoyu Chen^a, Yunlong Jiang^a, Cheng Feng^a and Chaochuang Yin^{b*}

a School of Mechanical Engineering & Urban Rail Transit, Changzhou University, Changzhou 213001, China.

b School of Chemistry and Materials Engineering, Liupanshui Normal University, Guizhou, 553004, China.

* Corresponding authors:

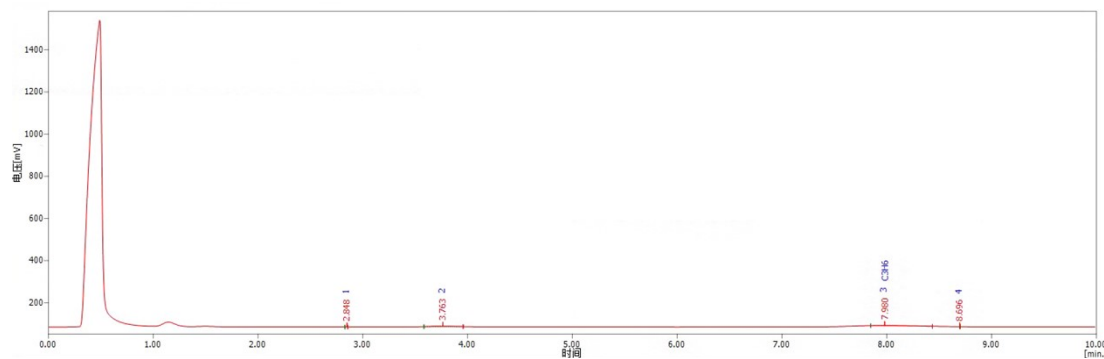
E-mail nizhijiang@cczu.edu.cn (Zhijiang Ni).
addresses: chaochuang@lpssy.edu.cn (Chaochuang Yin)

Total number of Pages: 17

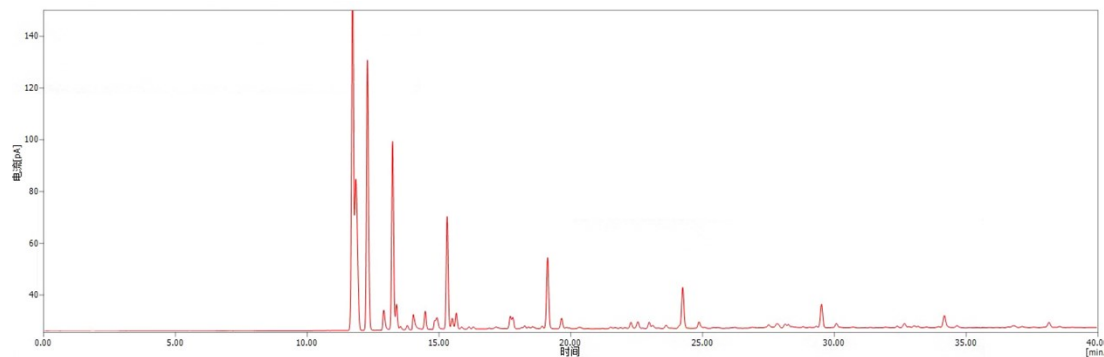
Total number of Figures: 7 (Fig. S1-Fig. S7)

Total number of Tables: 8 (Table S1-Table S8)

Carbon Balance Calculation:



(a) TCD signals in the channel 1



(b) FID signals in the channel 2

Fig. S1 Typical GC signals during CO₂ hydrogenation

Table S1 The test date of gas composition after reaction by TCD

Gas composition after reaction	<i>Correction factor f_(w)</i>
H2	0.0747
N2	1.0
CO	0.8561
CH4	0.2386
CO2	0.7432

Table S2 The test date of hydrocarbon composition after reaction by FID

Hydrocarbon composition after reaction	Correction factor <i>f_(w)</i>
C1	1
C2	0.4839964
C3	0.259133
C4	0.2011207
C5	0.115446
C6	0.115446
C7	0.115446
C8	0.115446
C9	0.115446

$$X_{CO_2} = \frac{n_{in,CO_2} - n_{out,CO_2}}{n_{in,CO_2}} = \frac{F_{in} \times f_{CO_2} \times A_{in,CO_2} - F_{out} \times f_{CO_2} \times A_{out,CO_2}}{F_{in} \times f_{CO_2} \times A_{in,CO_2}} = 1 - \frac{A_{in,N_2} \times A_{out,CO_2}}{A_{out,N_2} \times A_{in,CO_2}}$$

$$n_{in,CO_2} = \frac{A_{in,CO_2} \times f_{CO_2}}{A_{N_2} \times f_{N_2}} \times n_{N_2}$$

$$n_{out,CO_2} = \frac{A_{out,CO_2} \times f_{CO_2}}{A_{N_2} \times f_{N_2}} \times n_{N_2}$$

$$n_{out,CO} = \frac{A_{out,CO} \times f_{CO}}{A_{N_2} \times f_{N_2}} \times n_{N_2}$$

$$S_{CO} = \frac{n_{out,CO}}{n_{in,CO_2} - n_{out,CO_2}} = \frac{A_{in,N_2} \times A_{out,CO}}{A_{out,N_2} \times A_{in,CO_2} - A_{in,N_2} \times A_{out,CO_2}}$$

$$n_{CH_4} = \frac{A_{CH_4} \times f_{CH_4}}{A_{N_2} \times f_{N_2}} \times n_{N_2}$$

$$Carbon\ balance = \frac{n_{out,CO_2} + \sum_1^n C_i \times i + n_{out,CO}}{n_{in,CO_2}} \times 100$$

The SMSI strength Calculation:

The SMSI strength was quantified by integrating multiple characterization parameters through a weighted formula. The calculation steps are as follows:

Parameter Selection and Normalization

Three key parameters were selected based on their established correlation with SMSI effects:

Oxygen vacancy density ($O_v\%$): Determined from O 1s XPS peak deconvolution.

Reduction temperature shift (ΔT): Calculated as

$\Delta T = T_{ref} - T_{sample}$, where T_{ref} is the Fe_2O_3 reduction temperature of $FeNa/FeAl_2O_4$ ($428\text{ }^\circ C$) and T_{sample} is that of $FeNa/HEOs$ ($304\text{ }^\circ C$).

Fe^{3+} proportion ($Fe^{3+}\%$): Derived from Fe 2p XPS peak fitting (Fig. 4a).

Each parameter was normalized to a 0–100% scale using:

$$P_{norm} = \frac{P_{sample} - P_{min}}{P_{max} - P_{min}}$$

where P_{min} and P_{max} are the minimum and maximum values observed in the dataset (e.g., $O_v\%$: 18.07–37.93%).

The weights of parameters (α , β , γ) were assigned based on their relative contributions to SMSI, supported by literature and experimental data:

$O_v\%$ ($\alpha = 0.5$): Oxygen vacancies are critical for electron transfer at the metal-support interface, as demonstrated in SMSI systems like Pt/TiO_2 ¹.

ΔT ($\beta = 0.3$): Reduction temperature shifts reflect the thermodynamic facilitation of metal oxide reduction by SMSI².

$Fe^{3+}\%$ ($\gamma = 0.2$): Higher Fe^{3+} content indicates electron depletion from Fe to the support, a hallmark of electronic SMSI³.

The final SMSI strength (%) was calculated as:

$$SMSI = \alpha \cdot O_v\% + \beta \cdot \Delta T_{norm} + \gamma \cdot Fe^{3+}\%$$

where ΔT_{norm} is the normalized reduction temperature shift.

Based on the calculation formulas of P_{norm} and SMSI mentioned above, as well as the data of $Fe^{3+}\%$ and $O_v\%$ in supporting information Table S6, 7 and the reduction temperature in Fig. 4c of the main text, the SMSI values of each catalyst were calculated. The results are shown in Table S3.

Table S3 Calculated SMSI value

Catalyst	SMSI (%)
$FeNa/FeAl_2O_4$	30
$FeNa/FeCoCuZnMnAl_2O_4-2$	63.96
$FeNa/FeCoCuZnMnAl_2O_4-1$	80

Table S4 The catalytic performances of Fe-based catalysts in CO₂ hydrogenation.

Catalyst	CO ₂ Con(%)	Selectivity ^a (%)					O/P ^b	STY (mg/gcat·h)
		CH ₄	C ₂ ⁼ -C ₄ ⁼	C ₂ ⁰ -C ₄ ⁰	C ₅ +	CO		
FeNa/FeCoCu ZnMnAl ₂ O ₄ -2	36.93	30.72	37.01	9.47	22.96	4.37	3.91	85.47
FeNa/FeCoCu ZnMnAl ₂ O ₄ -1	40.03	31.25	39.28	8.59	20.93	5.51	4.57	98.78
FeNa/FeAl ₂ O ₄	38.32	44.07	14.21	27.85	14.03	9.53	0.51	27.77

Reaction conditions: 280 °C, 2.5 MPa, H₂/CO₂ = 3, GHSV=1650ml/(g*h), 100 h, Catalyst 0.4 g.^a Hydrocarbon selectivity was normalized with the exception of CO.^b O/P is the ratio of olefin (C₂⁼-C₄⁼) to paraffin (C₂⁰-C₄⁰).

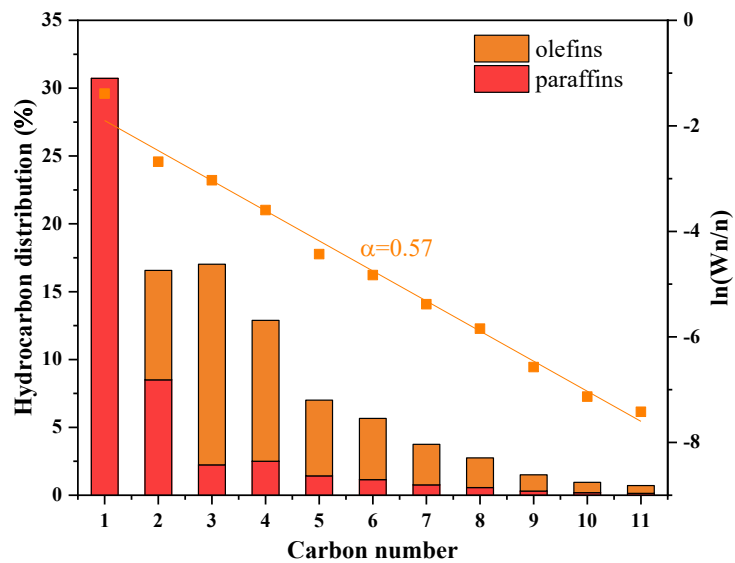


Fig. S2 The CO₂ hydrogenation performance on the FeNa/FeCoCuZnMnAl₂O₄-2 catalyst including the detailed hydrocarbons distribution and ln(W_n/n) values.

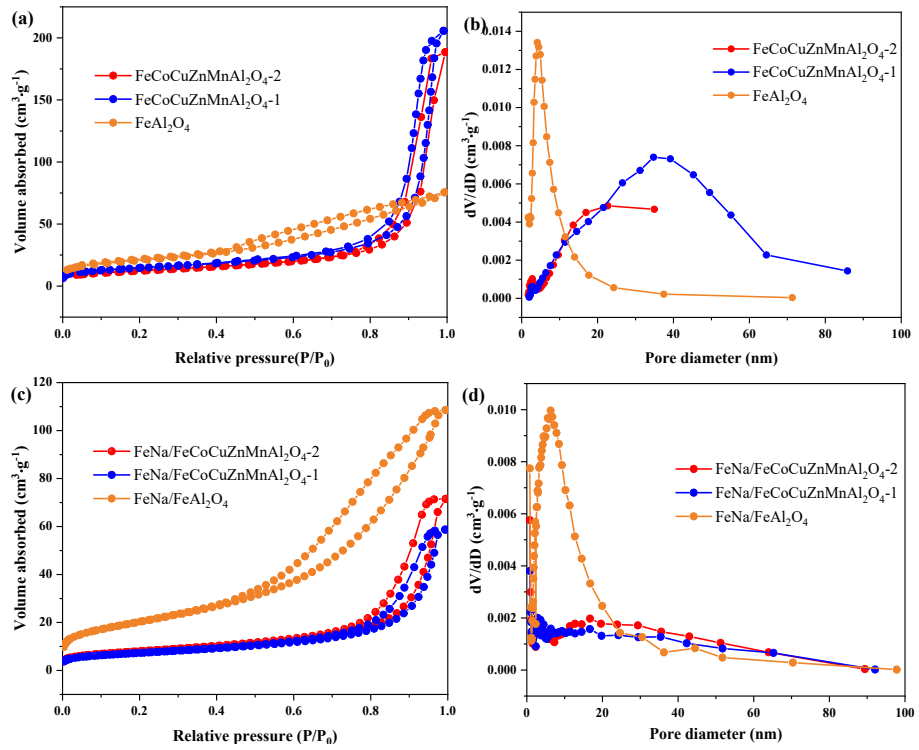


Fig. S3 N₂ adsorption isotherms of (a) FeAl₂O₄, FeCoCuZnMnAl₂O₄ supports and (b) their corresponding pore size distributions derived from the adsorption branches using the BJH algorithm. N₂ adsorption isotherms of (c) FeNa/FeAl₂O₄, FeNa/FeCoCuZnMnAl₂O₄, and (b) their corresponding pore size distributions derived from the adsorption branches using the BJH algorithm.

Table S5 Textural properties of supports and catalysts loaded with FeNa.

Catalyst	L(nm) FeAl ₂ O ₄ ^a	L(nm) Fe ₂ O ₃ ^b	S _{BET} ^c (m ² g ⁻¹)	D _p ^d (nm)	V _T ^e (cm ³ g ⁻¹)
FeCoCuZnMnAl ₂ O ₄ -2	8.07	-	43.66	22.55	0.23
FeCoCuZnMnAl ₂ O ₄ -1	9.7	-	51.9	27.37	0.32
FeAl ₂ O ₄	5.07	-	72.22	6.65	0.11
FeNa/FeCoCuZnMnAl ₂ O ₄ -2	9.61	18.73	28.68	18.86	0.11
FeNa/FeCoCuZnMnAl ₂ O ₄ -1	10.03	16.39	26.22	17.33	0.09
FeNa/FeAl ₂ O ₄	-	27.58	73.45	9.08	0.16

^a Crystal size calculated by Scherrer equation using FeAl₂O₄ peak from XRD.^b Crystal size calculated by Scherrer equation using Fe₂O₃ peak from XRD.^c Total surface area calculated using the Brunauer-Emmet-Teller (BET) method.^d Average pore diameter calculated using the Barrett-Joyner-Halenda (BJH) method.^e Total pore volume calculated using the BJH method.

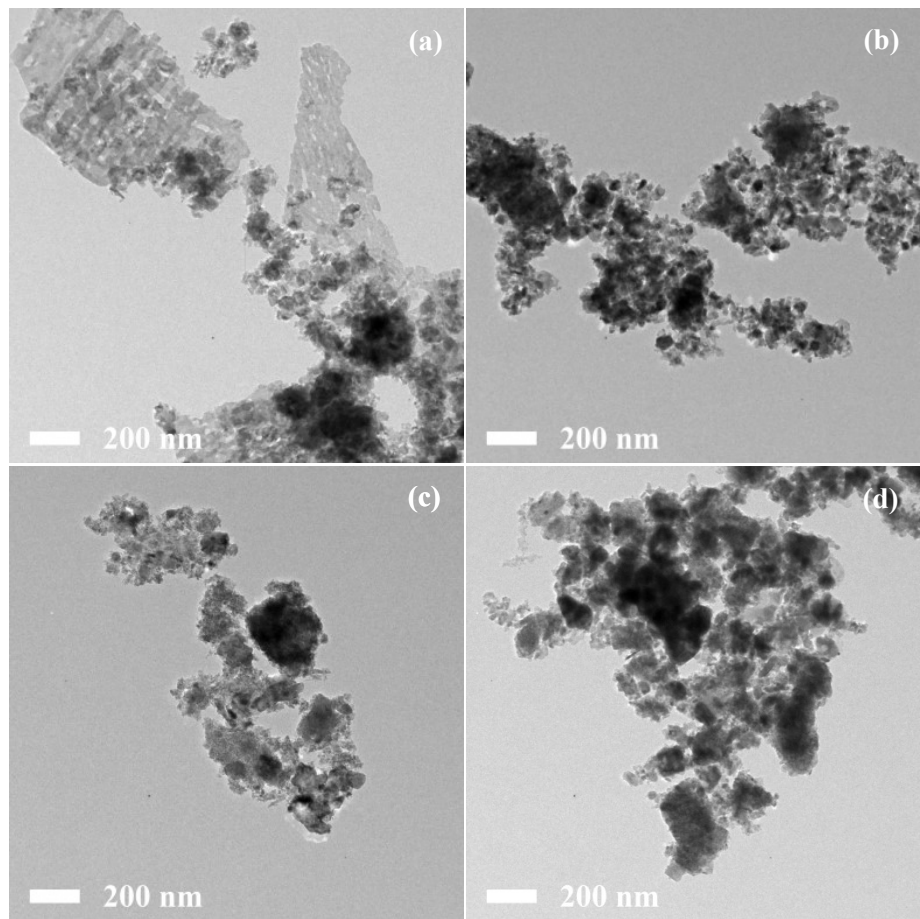


Fig. S4 TEM images of the fresh (a) FeNa/FeCoCuZnMnAl₂O₄-2, (b) FeNa/FeCoCuZnMnAl₂O₄-1, and (c) FeNa/FeAl₂O₄ catalyst. (d) TEM images of the spent FeNa/FeCoCuZnMnAl₂O₄-1 catalyst.

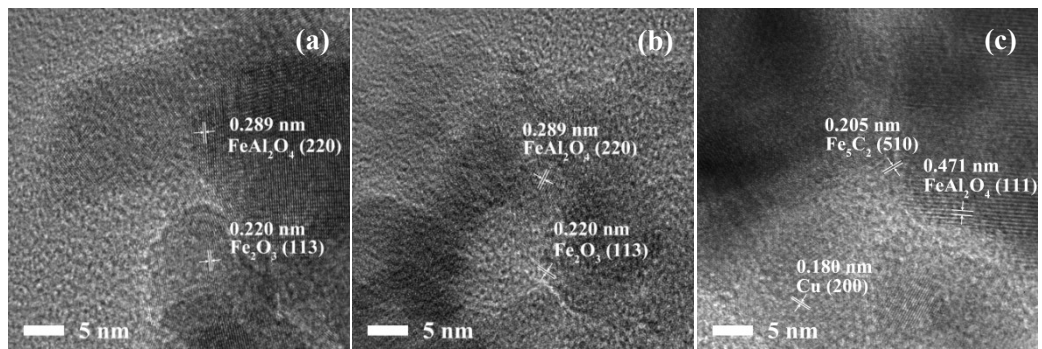


Fig. S5 HR-TEM images of the fresh (a) FeNa/FeCoCuZnMnAl₂O₄-2 and (b) FeNa/FeAl₂O₄ catalyst. (c) HR-TEM images of the spent FeNa/FeCoCuZnMnAl₂O₄-1 catalyst.

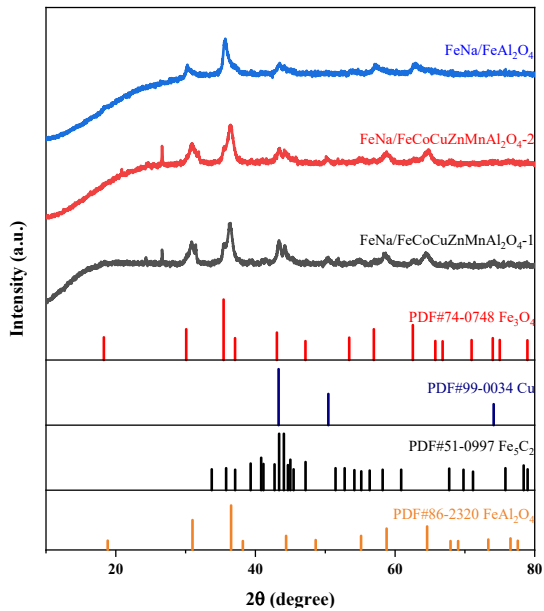


Fig. S6 XRD patterns of spent FeNa/FeAl₂O₄, FeNa/FeCoCuZnMnAl₂O₄-1 and FeNa/FeCoCuZnMnAl₂O₄-2 catalysts.

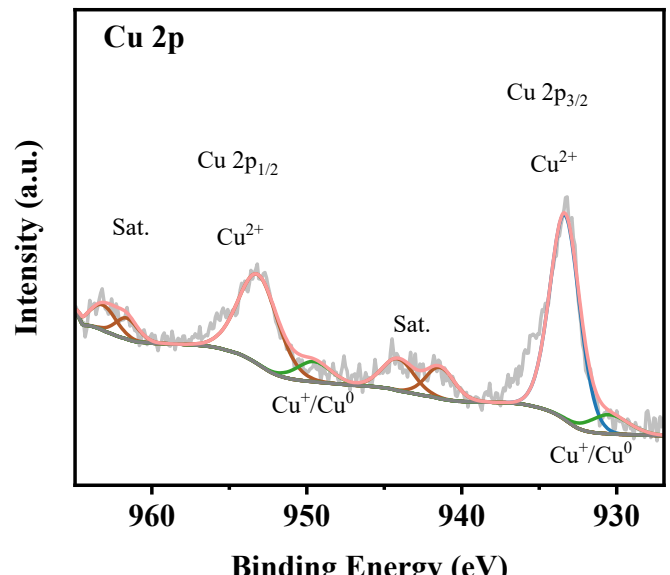


Fig. S7 XPS spectra of spent FeNa/FeCoCuZnMnAl₂O₄-1 catalyst in Cu2p region.

Table S6 The ratio peak area of the total peak area of the spent catalysts depends on the XPS spectra of Fe 2p.

Catalyst	Fe ³⁺ /(Fe ²⁺ +Fe ³⁺) (%)	Fe _x C _y /all (%)
FeNa/FeAl ₂ O ₄	39.47	6.96
FeNa/FeCoCuZnMnAl ₂ O ₄ -2	42.8	8.74
FeNa/FeCoCuZnMnAl ₂ O ₄ -1	43.99	9.71

Table S7 The O_v ratio peak area of the total peak area of the fresh and spent catalysts depends on the XPS spectra of O 1s.

Catalyst	fresh (%)	spent (%)
FeNa/FeAl ₂ O ₄	18.07	33.32
FeNa/FeCoCuZnMnAl ₂ O ₄ -2	35.89	45.05
FeNa/FeCoCuZnMnAl ₂ O ₄ -1	37.93	35.12

Table S8 The amount of CO₂ and H₂ desorbed in the CO₂-TPD or H₂-TPD profiles of the Fe-based catalysts.

Samples	The amount of CO ₂ desorbed (μmol/g)			The amount of H ₂ desorbed (μmol/g)
	Total	α peak	β peak	
FeNa/FeAl ₂ O ₄	99	52	47	470
FeNa/FeCoCuZnMnAl ₂ O ₄ -2	96	89	7	228
FeNa/FeCoCuZnMnAl ₂ O ₄ -1	97	32	65	348

References

- (1) Tauster, S. J.; Fung, S. C.; Garten, R. L. Strong Metal-Support Interactions. Group 8 Noble Metals Supported on Titanium Dioxide. *J. Am. Chem. Soc.* 1978, 100 (1), 170–175. <https://doi.org/10.1021/ja00469a029>.
- (2) Qiao, L.; Wang, X.; Zong, S.; Huang, Z.; Zhou, Z.; Fan, M.; Yao, Y. Anion-Doping-Mediated Metal–Support Interactions in CeO₂ -Supported Pd Catalysts for CO₂ Hydrogenation. *ACS Catal.* 2024, 14 (17), 13181–13194. <https://doi.org/10.1021/acscatal.4c02874>.
- (3) Wang, W.; Huo, K.; Wang, Y.; Xie, J.; Sun, X.; He, Y.; Li, M.; Liang, J.; Gao, X.; Yang, G.; Lin, S.; Cao, F.; Jiang, H.; Wu, M.; Tsubaki, N. Rational Control of Oxygen Vacancy Density in In₂O₃ to Boost Methanol Synthesis from CO₂ Hydrogenation. *ACS Catal.* 2024, 14 (13), 9887–9900. <https://doi.org/10.1021/acscatal.4c01929>.